International Journal of Agriculture, Environment and Food Sciences

JAEFS

e-ISSN : 2618-5946

DOI: 10.31015/jaefs.2020.1.5

www.jaefs.com

Research Article

Int J Agric Environ Food Sci 4 (1): 27-38 (2020)

Artificial neural network application for forecasting the nitrogen oxides in the atmosphere at the microclimate conditions: example of Iğdır city in Turkey

Aysun Altikat[1,*]

[1]Iğdır University, Faculty of Engineering, Department of Environmental Engineering, Iğdır, Turkey

[*]Corresponding Author: aysun.altikat@igdir.edu.tr

Abstract

The aim of this research is forecasting the NO_x, NO_2 and NO concentration levels with different artificial neural networks structures (ANNs) and determining the best ANNs structure for forecasting emissions. For this aim, it was used one learning function and, six different transfer function pairs with three different neuron numbers. The MATLAB software helped constructing ANNs models. In addition, the air pollutants and meteorological factors were used as input parameters simultaneously at the ANNs. The end of the research, NO_x, NO and NO_2's concentration levels were modelled with high accurate levels. The R^2 values of the NO_x, NO and NO_2 were calculated as 0.998, 0.995 and 0.997, respectively. The best results were obtained from ANNs structures which used Logarithmic sigmoid - Symmetric sigmoid transfer functions with 20 and 30 neuron number for forecasting of the NO_x and NO concentration levels, respectively. In addition, the forecasting of NO_2 emission rate, the best results were determined from the ANNs structure used Logarithmic sigmoid - Linear transfer function with 30 neuron number. According to sensitivity analyses and correlation tests, it was concluded that O_3, SO_2, wind direction, wind speed, and relative humidity inputs were more effective on the NO_2, NO and NO_x concentrations than the other inputs. Finally, it can be said that with the use of both air pollutants and meteorological factors as input parameters simultaneously the artificial neural network models can be simulated the concentration level of NO, NO_x and NO_2 with high accuracy.

Keywords: Air pollutions, Meteorological factor, ANN, Transfer function, Learning function

Introduction

The atmospheric pollution, which impairs on the respiratory and cardiovascular system, is an important factor both environmental conditions and human health, so it should be continuously controlled and observed (Zhang et al., 2012). Generally, pollutant emissions and meteorological factors affect the air pollution level. Some of the researchers, which aimed determining reasons the air pollutant, stated that the air pollution was influenced negatively by atmospheric pollutants (Gantt et al., 2010; Urbanski et al., 2011; Gao et al., 2014) while the others stated that it was affected by meteorological factors. (Wang et al., 2013; Wang et al., 2014 a; Wu et al., 2014 b; Russo et al., 2015).

NO_x has an important role in terms of the air pollution. NO_x affects both air pollution and human health so causes diseases such as pulmonary edema and damaged central nervous system, tissue, etc. (Lal and Patil, 2001). In addition, NO_x undergoes various complex reactions to generate several secondary pollutants which are known to be even more harmful than their precursor.

The forecasting of the air pollution is an important issue in the terms of both environmental pollution evaluations and precautions for countries' air pollution situation in the future. So, lots of researches have been done for modelling with statistical methods of air pollution levels, and in these researches generally examined the relationship among the air pollutants (Ozel and Cakmakyapan, 2015). In addition, autoregressive integrated moving average model (Samia et al., 2012; Jian et al., 2012), artificial neural network (Chaudhuri and Acharya, 2012; Elangasinghe et al., 2014; Feng et al., 2015; Pauzi and Abdullah, 2015; Zhang et al., 2017), community multi-scale air quality model (Chen et al., 2014;Wu et al., 2014a; Djalalova et

Cite this article as:
Altikat, A. (2020). Artificial neural network application for forecasting the nitrogen oxides in the atmosphere at the microclimate conditions: example of Iğdır city in Turkey. Int. J. Agric. Environ. Food Sci., 4(1), 27-38
DOI: https://dx.doi.org/10.31015/jaefs.2020.1.5
ORCID: [1]0000-0001-9774-2905
Received: 19 October 2019 **Accepted:** 27 January 2020 **Published Online:** 06 March 2020
Year: 2020 **Volume:** 4 **Issue:** 1 (March) **Pages:** 27-38
Available online at : http://www.jaefs.com - http://dergipark.gov.tr/jaefs
Copyright © 2020 International Journal of Agriculture, Environment and Food Sciences (Int. J. Agric. Environ. Food Sci.)
This is an open access article distributed under the terms of the Creative Commons Attribution 4.0 International (CC-by 4.0) Licens

al., 2015), fuzzy inference system (Domannska and Woktylak, 2012), grey model (Pai et al., 2013), and other hybrid methods (Chen et al., 2013; Corporation, 2013; Russo and Soares, 2014; Yahya et al., 2014) can be listed which using methods for modelling air pollution levels.

Feed forward back propagation (FFBP) generally used in the ANN. An FFBP has the presence of one or more hidden layers, whose computation nodes are correspondingly called hidden neurons of the hidden units. The function of hidden neurons is to intervene between the external input and the network output in some useful manner. By adding one or more hidden layers, the network is able to extract higher order statistics. The ability of hidden neurons to extract higher order statistics is particularly valuable when the size of the input layer is large. The source nodes in the input layer of the network supply respective elements of the activation pattern (input vector), which constitute the input signals applied to the neurons (computation nodes) in the second layer (i.e. the first hidden layer). The output signals of the second layer are used as inputs to the third layer, and so on for the rest of the network. Typically, the neurons in each layer of the network have as their inputs the output signals of the preceding layer only. The set of the output signals of the neurons in the output layer of the network constitutes the overall response of the network to the activation patterns applied by the source nodes in the input (first) layer. The FFBP are trained using the LM optimization technique. This optimization technique is more powerful than the conventional gradient descent techniques (Cigizoglu and Kisi 2005).

The aim of this study is to model atmospheric NO_x, NO and NO_2 emissions with different artificial neural network structures in microclimate atmospheric conditions in Iğdır/Turkey. Iğdır is adjacent to Iran, Nakhichevan and Armenia. In addition, the Metsamor nuclear power plant in Armenia is only 16 km from the border of Iğdır city. The level of air pollution is quite high throughout the year. For this purpose, 18 different artificial neural structures (ANNs) were examined with different transfer functions and neural numbers. Unlike the other studies, in this research, as input parameters not only atmospheric pollutants (SO_2, O_3, NO, NO_2, NO_x and PM_{10}) but also meteorological factors (relative humidity, air pressure, air temperature, wind direction and wind speed) were used at the ANNs models.

Materials and Methods

In the research, it was used the atmospheric and meteorological data which obtained by Turkey Ministry of Environment and Urbanization / National Air Quality Monitoring between the 01/102016 - 06/11/2018 in Iğdır city. The detail data of pollutants and meteorological factors are plotted in figure 1 and figure 2, respectively. Data were divided into three parts as 70% for training, 15% for cross validation, and 15% for testing to prevent overfitting. For prediction the NO_x, NO and NO_2 emissions, 18 different artificial neural network structures were used with different transfer functions and neurons numbers. The input and output parameters which used in the ANNs structures have been illustrated in the table 1 and ANNs structure was illustrated figure 3. In the research one learning function, six different transfer function combinations and 3 different numbers of neurons were used in the artificial neural structures (ANNs). The architecture of the ANNs model was given table 2. The studied network was implemented under MATLAB 7.10 (the MathWorks, Inc. Natick,MA,USA software), with the Neural Network Toolbox 4 (Maltlab, 2015).

Table 1. The input and output parameters for forecasting of NO_x, NO and NO_2

Forecasting NO_x		Forecasting NO		Forecasting NO_2	
Input	Output	Input	Output	Input	Output
S_O2		SO_2		SO_2	
NO		NOx		NO	
O_3		O_3		O_3	
NO_2		NO_2		NOx	
PM_{10}	NO_x	PM_{10}	NO	PM_{10}	NO_2
rh		rh		rh	
ap		ap		ap	
at		at		at	
wd		wd		wd	
ws		ws		ws	

rh: Relative humidity (%); ap: Air pressure (mbar); at: Air temperature (°C); wd: Wind direction (degree); ws: Wind speed ($m \cdot s^{-1}$).

Table 2. Functions and neurons numbers used in the ANNs

Learning function	Transfer functions	Neurons
Levenberg-Marquardt (trainlm)	Logsig-logsig	10
	Purelin-purelin	
	Tansig-tansig	20
	Logsig-pureline	
	Logsig-tansig	30
	Pureline-tansig	

logsig: Logarithmic sigmoid transfer function, purelin: linear transfer function; tansig: symmetric sigmoid transfer function

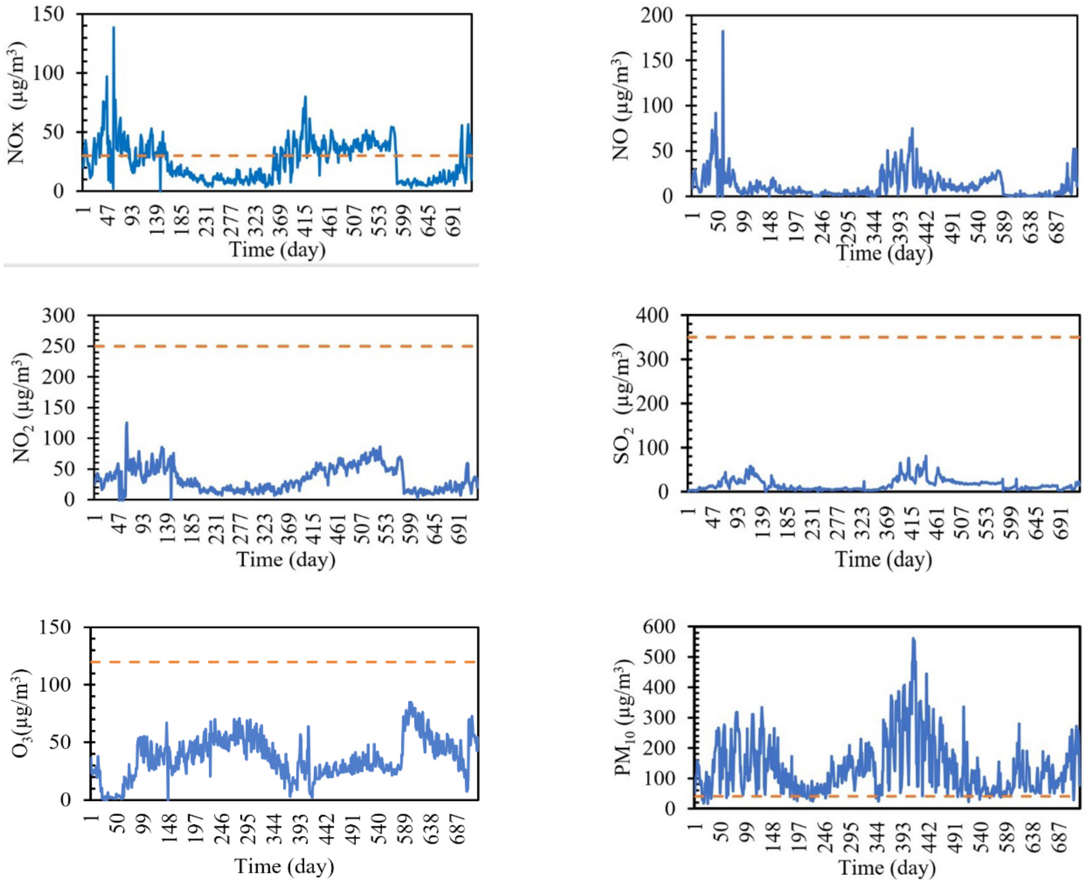

Figure 1. Air pollutant concentrations 1/10/2016-30/10/2018 horizontal line refers to the daily legal limits

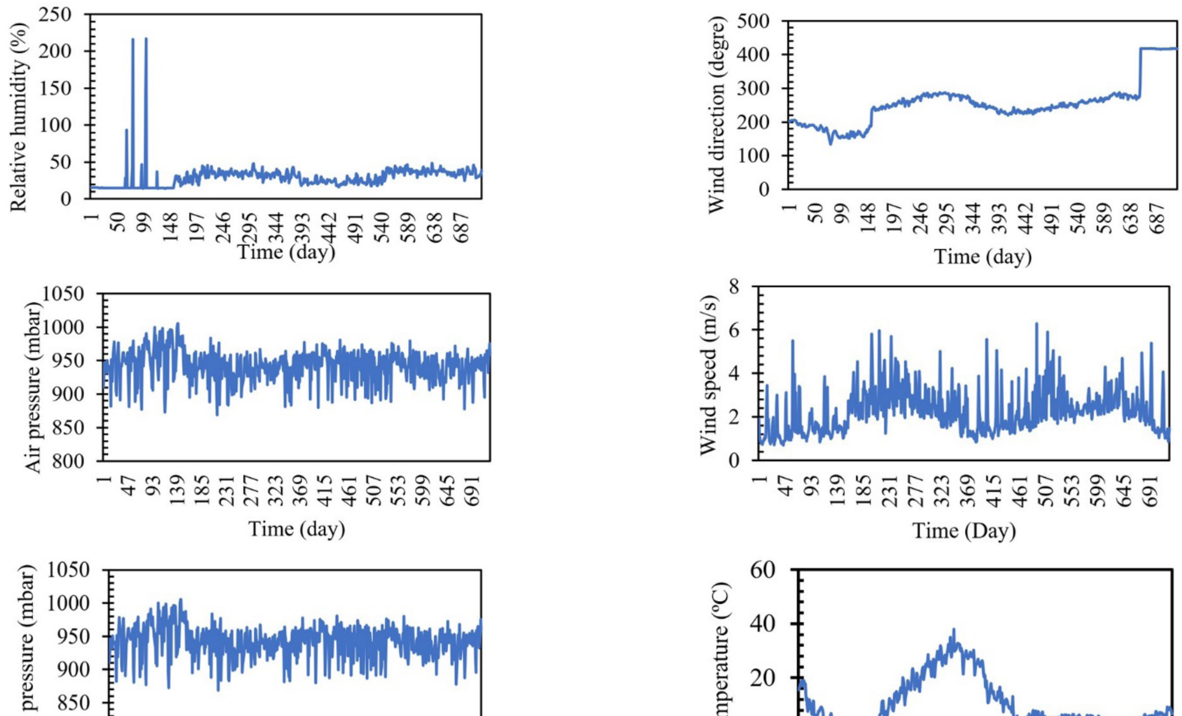

Figure 2. Meteorological factors 1/10/2016-30/10/2018

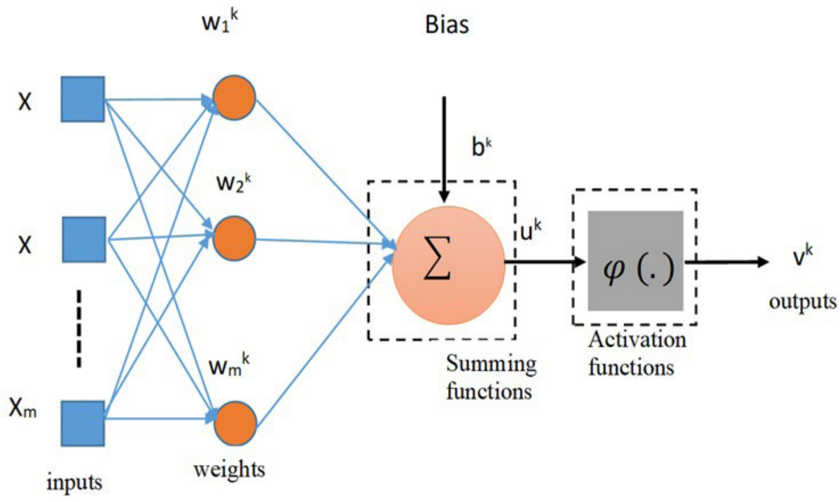

Figure 3. ANNs structure

Correlation tests

In order to determine the relationship between the inputs parameters and NO_x, NO, NO_2, firstly, the distribution of the data was examined. For this purpose, SPSS statistics program was used. As a result of the analyzes, it was determined that both inputs parameters and NO_x, NO and NO_2 concentrations determined a non-parametric distribution. These data were then subjected to correlation tests. The data didn't show a linear distribution, for this reason, Spearman's correlation tests were used. Correlation coefficients were taken into consideration in the interpretation of the test. The relationship between the factors with a correlation coefficient of less than 0.5 was considered as the weak correlation, and if this value was between 0.5 and 0.7, it was concluded that the change between the factors was moderately correlated. If the correlation coefficient is greater than 0.7, it was consideration a high correlation between the factors (Zou et al., 2003).

Sensitivity Analyzing

To appoint how much significant the input parameters are, the weight matrices and Garson equation (eq. 1) were used (Aleboyeh et al., 2008). In the equation Ij is percentage of the relative importance of the jth input variable on the neurons and W^{ih} and W^{ho} are the matrices of weights between input-hidden layer and hidden-output layer respectively, N is the total number of neurons in the corresponding layer, respectively, and subscripts 'k', 'm' and 'n' are indices referring to the neurons in input, hidden and output layers, respectively.

$$I_j = \frac{\sum_{m=1}^{Nh}\left(\left(\left|W_{jm}^{ih}\right| / \sum_{k=1}^{Ni}\left|W_{km}^{ih}\right|\right) \times \left|W_{mn}^{ho}\right|\right)}{\sum_{k=1}^{Ni}\left\{\sum_{m=1}^{Nh}\left(\left|W_{km}^{ih}\right| / \sum_{k=1}^{Ni}\left|W_{km}^{ih}\right|\right) \times \left|W_{mn}^{ho}\right|\right\}} \quad \ldots\ldots(1)$$

Performance evaluation

The performance of constructed ANNs models was statistically measured, in terms of the mean square error (RMSE) (eq.2), mean absolute error (MAE) (eq.3) and coefficient of determination (R^2) (eq.4). The model is considered accurate when R^2 is close to 1.0, while RMSE must be as small as possible. MAE is a measure used to evaluate how close the estimates are to the observed (real) results. In these equations; where, n is the number of data, Ypi is the predicted value from observation i, Ydi is the real value from observation i, and $\bar{Y}$ is the average of the observed values.

$$RMSE = \sqrt{\frac{1}{n}\sum_{i=1}^{n}\left(Y_{pi} - Y_{di}\right)^2} \quad \ldots\ldots(2)$$

$$MAE = \frac{1}{n}\sum_{i=1}^{n}\left|Y_{pi} - Y_{di}\right| \quad \ldots\ldots(3)$$

$$R^2 = 1 - \left(\frac{\sum_{i=1}^{n}\left(Y_{pi} - Y_{di}\right)^2}{\sum_{i=1}^{n}\left(Y_{pi} - \bar{Y}\right)^2}\right) \quad \ldots\ldots(4)$$

Results and Discussions

Results of correlation tests

In order to determine the relationship between the inputs parameters and NO_x, NO, NO_2 the distribution of the data were given in the table 3. When the correlation coefficients are analyzed, it is seen that the effects of other pollutant gases on NO_x, NO and NO_2 are more effective than atmospheric conditions. In addition to, among the atmospheric conditions, wd, ws and at were determined to be more effective on NO_x, NO and NO_2.

Table 3 The results of Spearman's correlation test

NOx		NO		NO_2	
NO	0.907	NO_X	0.907	NO_X	0.899
NO_2	0.899	O_3	-0.741	NO	0.704
O_3	-0.695	NO_2	0.704	SO_2	0.665
SO_2	0.643	SO_2	-0.597	O_3	-0.571
wd	-0.578	wd	-0.536	wd	-0.563
ws	-0.537	ws	0.528	rh	-0.506
wt	0.501	at	0.514	at	0.416
rh	-0.500	PM_{10}	0.432	ws	-0.386
PM10	0.398	rh	-0.424	ap	0.288
ap	0.333	ap	0.308	PM_{10}	0.268
NO_X	1	NO	1	NO_2	1

rh: Relative humidity; ap: Air pressure; at: Air temperature; wd: Wind direction; ws: Wind speed.

Results of Prediction NO_x emissions

The artificial neural networks structures and their statistical results for prediction of NO_x emissions was given in table 4a. When examined the statistical results, it can be seen the highest R^2 (0.998) and lowest MAE (0.007) values were obtained from the ANN 11 structure. In this structure with 30 neurons it was used Levenberg-Marquardt and Logarithmic sigmoid - Symmetric sigmoid as learning and transfer functions, respectively.

The ANN 11 structure's training, test and validation graphs were illustrated in the figure 4b. As can be seen from figure 4, the training, test and validation's R values are higher than 0.99. According these results it can be said that the network performance has high accuracy level. This high accuracy level can be understood from the figure 5 as well.

Table 4. The statistical results of different ANN structure for NO_x concentration

Model	Learning function	Transfer function	Number of neurons	RMSE	MAE	R^2
ANN 1	trainlm	Logsig-logsig	10	0.680	0.640	0.005
ANN 2	trainlm	Purelin-purelin	10	0.019	0.007	0.994
ANN 3	trainlm	Tansig-tansig	10	0.033	0.022	0.982
ANN 4	trainlm	Logsig-pureline	10	0.017	0.010	0.995
ANN 5	trainlm	Logsig-tansig	10	0.014	0.007	0.997
ANN 6	trainlm	Pureline-tansig	10	0.041	0.032	0.974
ANN 7	trainlm	Logsig-logsig	20	0.680	0.640	0.013
ANN 8	trainlm	Purelin-purelin	20	0.019	0.008	0.994
ANN 9	trainlm	Tansig-tansig	20	0.022	0.013	0.992
ANN 10	trainlm	Logsig-pureline	20	0.012	0.008	0.998
ANN 11	trainlm	Logsig-tansig	20	0.011	0.007	0.998
ANN 12	trainlm	Pureline-tansig	20	0.042	0.032	0.972
ANN 13	trainlm	Logsig-logsig	30	0.680	0.640	0.000
ANN 14	trainlm	Purelin-purelin	30	0.020	0.008	0.994
ANN 15	trainlm	Tansig-tansig	30	0.018	0.010	0.994
ANN 16	trainlm	Logsig-pureline	30	0.016	0.007	0.996
ANN 17	trainlm	Logsig-tansig	30	0.015	0.009	0.996
ANN 18	trainlm	Pureline-tansig	30	0.041	0.031	0.973

trainlm: Levenberg-Marquardt; logsig: Logarithmic sigmoid transfer function; pureline: Linear transfer function; tansig: Symmetric sigmoid transfer function

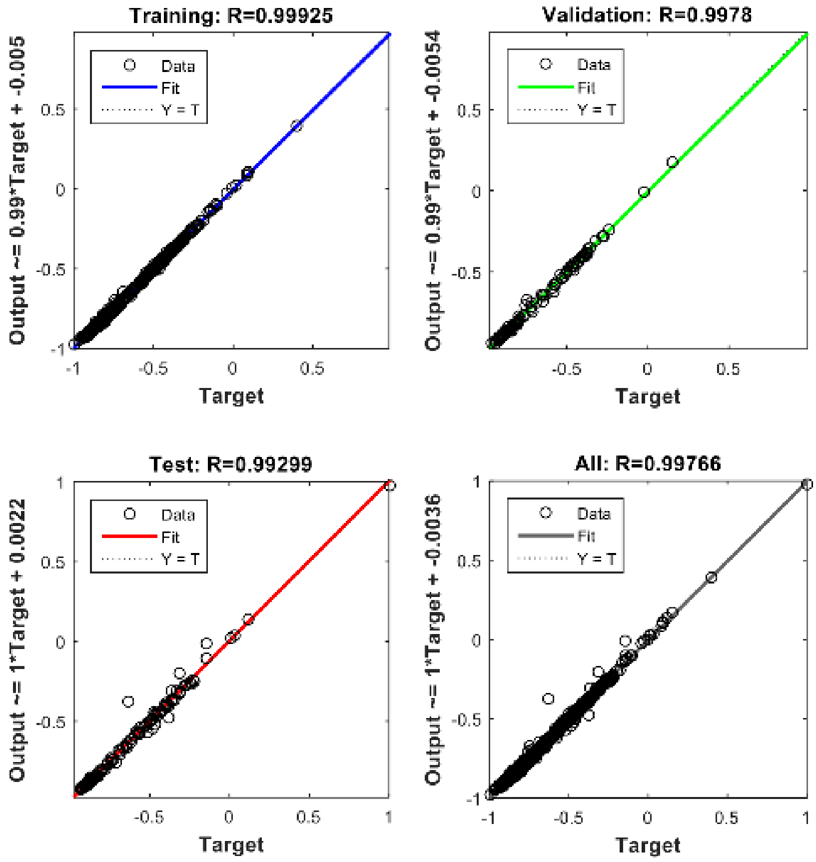

Figure 4a. The ANN 11 structure's network performance for forecasted NO_x emission

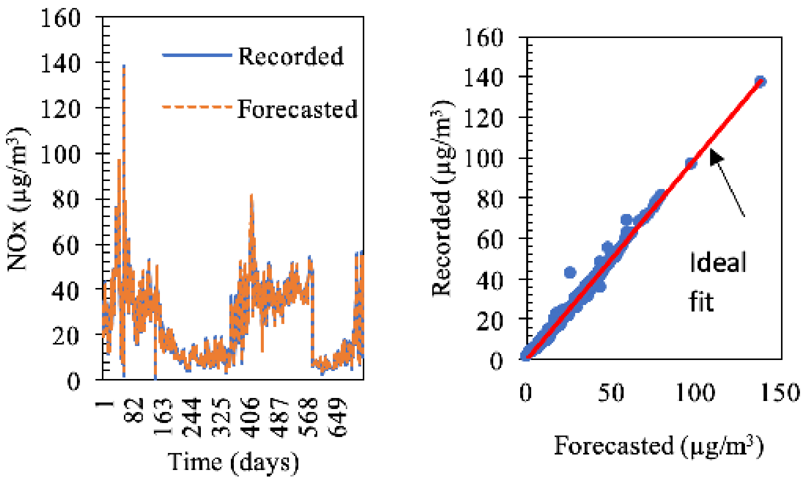

Figure 4b. Recorded and forecasted values for NO_x emission in the ANN 11 structure

Result of Prediction of NO emissions

The statistical results for forecasted of NO concentration can be seen at the table 5. The best statistical results among the ANN structures was obtained at the ANN 17 structure. In the ANN 17 structure the R^2 and MAE value were calculated as 0.995 and 0.006, respectively, and also, this structure used learning and transfer functions as Levenberg-Marquardt, Logarithmic sigmoid- Symmetric sigmoid respectively, with 30 neurons. The ANN 17's network performance can be also seen in the figure 5. The R^2 values of the training, validation and test are 0.998, 0.990 and finally 0.987, respectively. Figure 6 illustrated that, the recorded and forecasted values of NO emission in the ANN 17 structure. As it can be seen at the figure 6, the NO concentration was modelled with high significance level with the ANN 17 structure.

Table 5. The statistical results of different ANN structure NO

Model	Adaption learning function	Transfer function	Number of hidden neurons	RMSE	MAE	R^2
ANN 1	trainlm	Logsig-logsig	10	0.741	0.848	0.189
ANN 2	trainlm	Purelin-purelin	10	0.000	0.007	0.985
ANN 3	trainlm	Tansig-tansig	10	0.001	0.011	0.976
ANN 4	trainlm	Logsig-pureline	10	0.000	0.007	0.986
ANN 5	trainlm	Logsig-tansig	10	0.000	0.012	0.982
ANN 6	trainlm	Pureline-tansig	10	0.001	0.008	0.980
ANN 7	trainlm	Logsig-logsig	20	0.742	0.850	0.223
ANN 8	trainlm	Purelin-purelin	20	0.000	0.008	0.985
ANN 9	trainlm	Tansig-tansig	20	0.000	0.005	0.994
ANN 10	trainlm	Logsig-pureline	20	0.000	0.010	0.988
ANN 11	trainlm	Logsig-tansig	20	0.001	0.016	0.977
ANN 12	trainlm	Pureline-tansig	20	0.001	0.016	0.978
ANN 13	trainlm	Logsig-logsig	30	0.742	0.850	0.009
ANN 14	trainlm	Purelin-purelin	30	0.000	0.008	0.985
ANN 15	trainlm	Tansig-tansig	30	0.000	0.007	0.992
ANN 16	trainlm	Logsig-pureline	30	0.000	0.009	0.989
ANN 17	trainlm	Logsig-tansig	30	0.000	0.006	0.995
ANN 18	trainlm	Pureline-tansig	30	0.000	0.009	0.991

trainlm: levenberg-marquardt; logsig: logarithmic sigmoid transfer function; pureline: Linear transfer function; tansig: Symmetric sigmoid transfer function

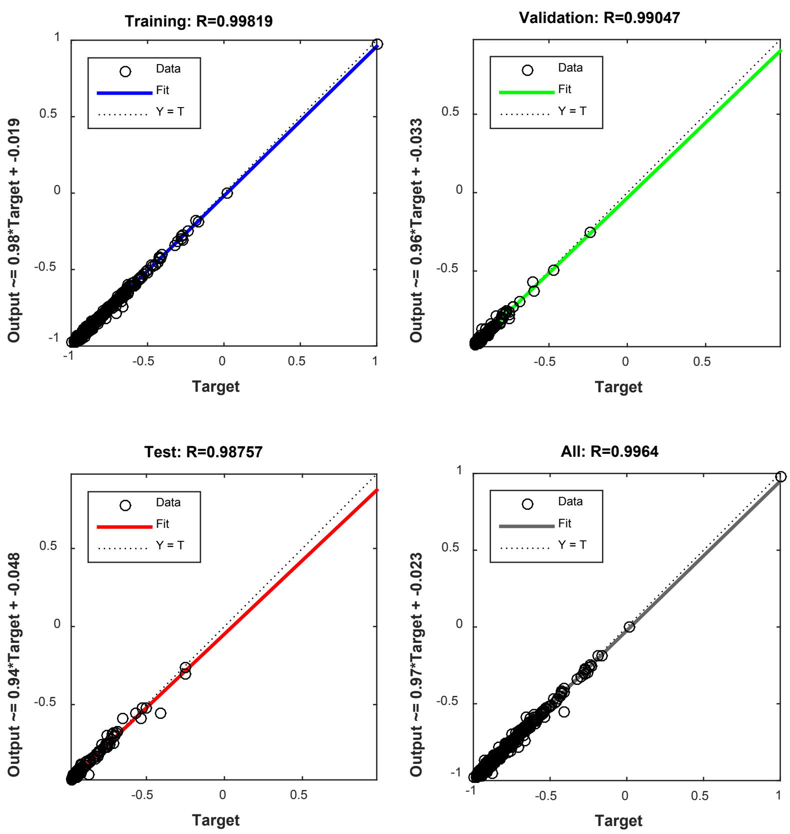

Figure 5. The ANN 17 structure's network performance for prediction NO emission

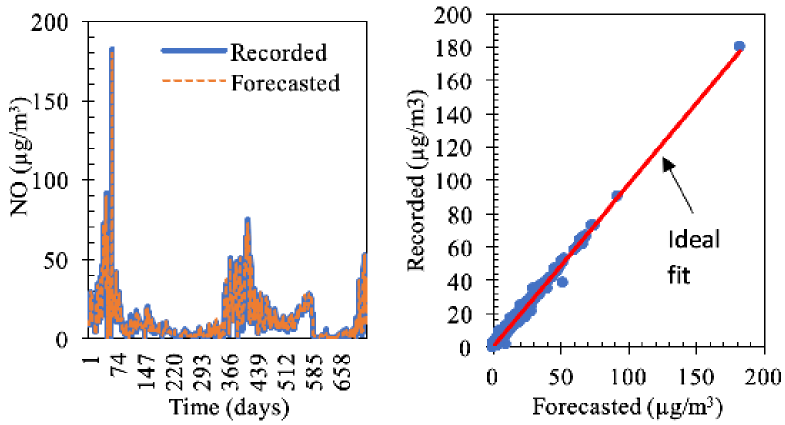

Figure 6. Observed and predicted values for NO emission in the ANN 17 structure

Results of Prediction NO_2 emission

In the research the NO_2 emission values was predicted with high accuracy level (R^2: 0.997, MAE:0.009) at the ANN 16 structure (Table 6). In this structure the learning and transfer functions were used as Levenberg-Marquardt and Logarithmic sigmoid – Linear, respectively with 30 neurons. When examined the ANN 16 structure's network performance it can be seen that high R^2 values such as 0.999, 0.993 and 0.992 for training, validation and test results, respectively (Figure 7). As shown at the figure 8, the NO_2 concentration was modelled with high significance level with the ANN 16 structure.

Table 6. The statistical results of different ANN structure NO_2

Model	Adaption learning function	Transfer function	Number of hidden neurons	RMSE	MAE	R^2
ANN 1	trainlm	Logsig-logsig	10	0.526	0.454	0.003
ANN 2	trainlm	Purelin-purelin	10	0.041	0.018	0.984
ANN 3	trainlm	Tansig-tansig	10	0.037	0.017	0.987
ANN 4	trainlm	Logsig-pureline	10	0.028	0.017	0.992
ANN 5	trainlm	Logsig-tansig	10	0.031	0.019	0.991
ANN 6	trainlm	Pureline-tansig	10	0.042	0.028	0.983
ANN 7	trainlm	Logsig-logsig	20	0.524	0.452	0.040
ANN 8	trainlm	Purelin-purelin	20	0.044	0.022	0.981
ANN 9	trainlm	Tansig-tansig	20	0.030	0.018	0.991
ANN 10	trainlm	Logsig-pureline	20	0.021	0.013	0.996
ANN 11	trainlm	Logsig-tansig	20	0.025	0.015	0.994
ANN 12	trainlm	Pureline-tansig	20	0.042	0.028	0.983
ANN 13	trainlm	Logsig-logsig	30	0.520	0.439	0.296
ANN 14	trainlm	Purelin-purelin	30	0.041	0.016	0.983
ANN 15	trainlm	Tansig-tansig	30	0.025	0.016	0.994
ANN 16	trainlm	Logsig-pureline	30	0.019	0.009	0.997
ANN 17	trainlm	Logsig-tansig	30	0.037	0.020	0.987
ANN 18	trainlm	Pureline-tansig	30	0.042	0.028	0.983

trainlm: Levenberg-Marquardt; logsig: logarithmic sigmoid transfer function; pureline: linear transfer function; tansig: Symmetric sigmoid transfer function.

Results of Sensitivity analyses

The weights used in determining the relative important of the input and output values were given in table 7. In addition, the results of the sensitivity analysis were illustrated at the figure 9, figure 10 and figure 11 for NO_x, NO and NO_2, respectively.

When examined the figures, the effects of pollutant gases for NO_x, NO and NO_2 were determined more effective than atmospheric conditions. The most effective pollutant gases in NO_x modeling were determined as NO, NO_2, O_3 and SO_2. In addition, the most effective atmospheric conditions in the NOx model were calculated as wd, ws, at and rh (Figure 8). Similar results were obtained in NO and NO_2 models (Figure 9, Figure 10). When examined the correlation test it can be seen that similar results.

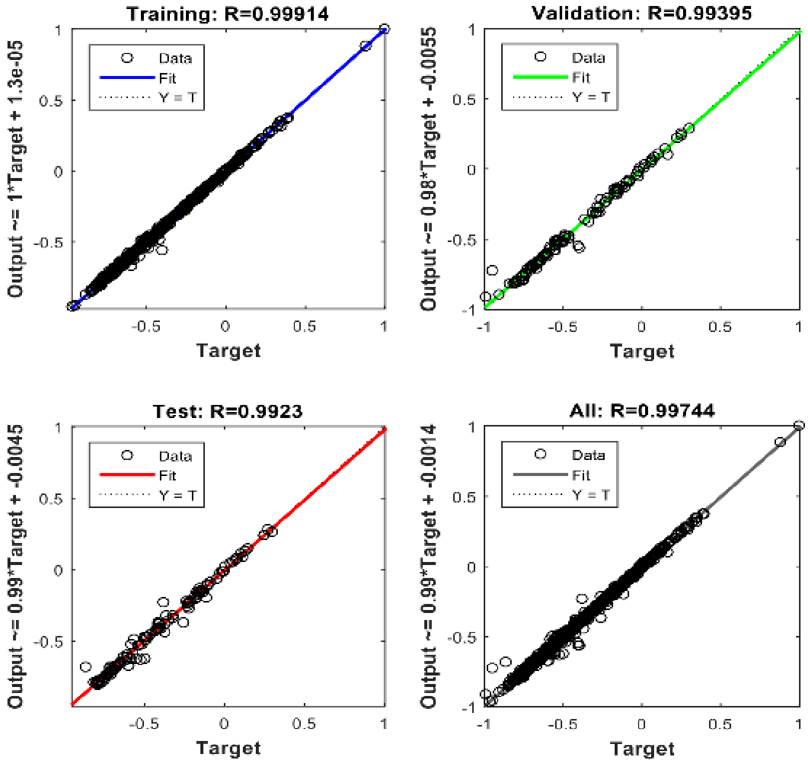

Figure 7. The ANN 16 structure's network performance for prediction NO_2 emission

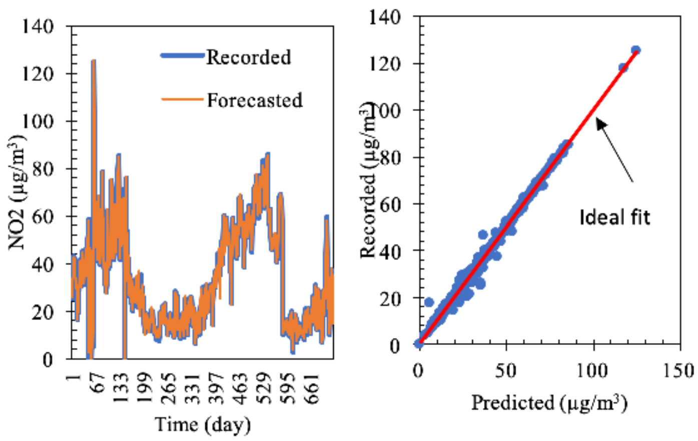

Figure 8. The ANN 16 structure's network performance for prediction NO_2 emission

Table 7. The weights between input and output values for NO_x, NO and NO_2

				W^{ih}						W^{ho}
rh	wd	ap	ws	at	SO_2	NO_2	NO	O_3	PM_{10}	NOx
0.81	2.72	0.46	0.34	0.88	-0.88	-0.19	-4.46	-0.07	1.56	-3.9
				W^{ih}						W^{ho}
rh	wd	ap	ws	at	SO_2	NO_X	O_3	NO_2	PM_{10}	NO
0.36	1.53	-0.22	0.99	0.54	1.55	-1.92	1.68	1.81	0.47	-0.22
				W^{ih}						W^{ho}
rh	wd	ap	ws	at	SO_2	NO_X	NO	O_3	PM_{10}	NO_2
-0.71	0.83	0.53	-0.60	0.63	-1.88	-2.51	-2.01	0.89	0.48	0.48

rh: Relative humidity; ap: Air pressure; at: Air temperature; wd: Wind direction; ws: Wind speed

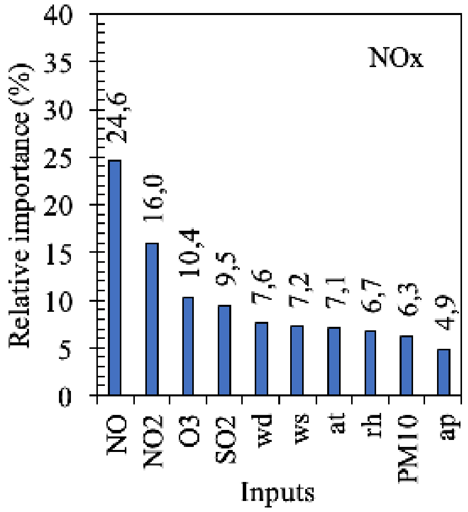

Figure 9 Relative importance values for NOx at the ANN 11 structure

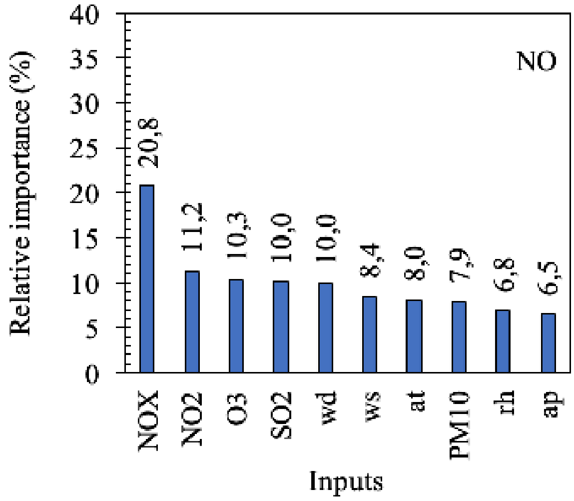

Figure 10 Relative importance values for NO at the ANN 17 structure

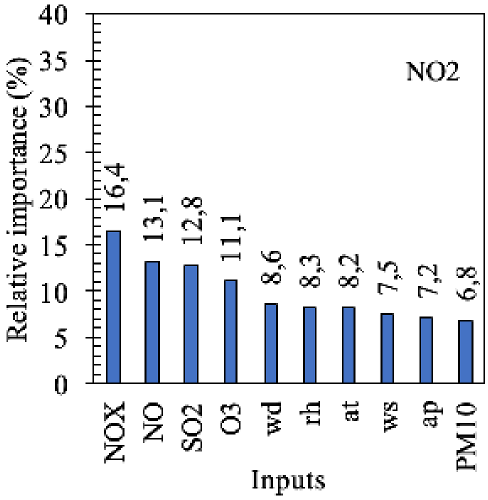

Figure 11 Relative importance values for NO at the ANN 16 structure

The main reason of nitrogen oxides emission (nitric oxide and nitrogen dioxide) is vehicle exhaust. Nitrogen dioxide forms as a result of reactions between the nitric oxide and ozone. (Gardner and Dorling, 1999). The amount of the air pollutant in the atmosphere are influenced by emission rate, chemical transformation and climate-atmospheric condition. Especially winds transport effects dispersion of pollutants. In addition, air temperatures are another important factor for NO_2 emission (Jiang et al., 2005).

The city of Iğdır where the research is conducted, located on the international road route. All the roads to Iran, Azerbaijan and Armenia pass through this city. In addition, Iğdır has microclimate properties. Due to its geographical location, there is not enough air circulation throughout the province. Therefore, the air pollution level throughout the province is quite high in all seasons of the year. The presence of large erosion sites in some districts of the province causes an increase in the level of particulate pollution. For these reasons, modeling of pollution throughout the province is very important in terms of future measures.

Artificial neural network has different learning rules and these effects the forecast accuracy. Chaudhuri and Acharya, (2012) studied effects of different learning rules in the ANN for forecasting concentration of atmospheric pollutants, and at the end of the research they determined non-linear perceptron model was better for forecasting the concentrations SO_2, CO and PM_{10}. However, for forecasting NO_2, delta learning is better than non-linear perceptron. Several researches have focused on the modelling air pollution with used ANN (Nagendra and Kahre,2006; Hrust et al., 2009; Kurt and Oktay, 2010; Cheng et al., 2012; Perez 2012; Wang et al., 2019; Alimissis et al., 2018). However, Elangasinghe et al., (2013) stated that at the forecasting studies the selection of the input parameters is very important for model performance, and different air pollutant used as input parameters is not enough high accuracy model. So, meteorological factors should be used together with air pollutants for high accuracy models (Singh et al, 2012; Yan Chan and Jian, 2013).

In this study, both meteorological factors and other air pollutants were used as input parameters, and obtained the best model performances (R^2>0.99) for NO_x, NO and NO_2 forecasting. Finally, it can be said that the ANN methods are very efficient for forecasting the air pollution concentration when the using appropriate input parameters.

Conclusion

The main objective of this research is to forecast the NO_x, NO and NO_2 concentration level in the atmosphere. For this purpose, 18 different ANNs structures were examined. In these structures, the one learning function (Levenberg-Marquardt) and six different transfer functions (logarithmic sigmoid - logarithmic sigmoid, linear - linear, Symmetric sigmoid - Symmetric sigmoid, logarithmic sigmoid - linear, logarithmic sigmoid - Symmetric sigmoid and Linear - Symmetric sigmoid) with three neuron (10,20,30) numbers were tested. In the networks, both meteorological factors (relative humidity, air pressure, air temperature, wind direction, wind speed) and air pollutants (SO_2, O_3, $PM_{10,}$ NO_x, NO and NO_2) were used as input parameters. At the end of the research, the NO_x, NO and NO_2 were modelled with high accuracy level (R^2>0.99). The best models for NO_x and NO concentration levels have been observed at the logarithmic sigmoid - symmetric sigmoid transfer functions with 20 and 30 neuron number, respectively. In addition, the best results have been determined from the ANNs structure which used Logarithmic sigmoid - Linear transfer function with 30 neuron number at the modelling of NO_2 concentration levels. In the sensitivity tests, it was concluded that O_3 SO_2, wd, ws, and rh inputs were more effective on the NO_2 NO and NO_x concentrations than other inputs. Similar results were obtained in the correlation tests.

Compliance with Ethical Standards

Conflict of interest

The author declared no potential conflicts of interest with respect to the research, authorship, and/or publication of this article.

Author contribution

The author read and approved the final manuscript. The author verifies that the Text, Figures, and Tables are original and that they have not been published before.

Ethical approval

Not applicable.

Funding

No financial support was received for this study.

Data availability

Not applicable.

Consent for publication

Not applicable.

References

Aleboyeh, A., Kasiri, M.B., Olya, M.E., Aleboyeh, H. (2008) Prediction of azo dye decolorization by UV/H2O2 using artificial neural networks. Dye. Pigment., 77,288-294. [Google Scholar].

Alimissis, A., Philippopoulos, K., Tzanis, C.G., Deligiorgi, D. (2018). Spatial estimation of urban air pollution with the use of artificial neural network models. Atmospheric Environment, 191, 2015-2013. [Google Scholar].

Chaudhuri, S., Acharya, R., (2012) Artificial neural network model to forecast the concentration of pollutants over Delhi: skill assessment of learning rules. Asian J. Water Environ. Pollut. 1, 71-81. [Google Scholar].

Chen, J., Lu, J., Avise, J.C., DaMassa, J.A., Kleeman, M.J., Kaduwela, A.P. (2014) Seasonal modeling of PM2.5 in California's San Joaquin Valley. Atmos. Environ. 92, 182-190. [Google Scholar].

Chen, Y., Shi, R., Shu, S., Gao, W. (2013) Ensemble and enhanced PM10 concentration forecast model based on stepwise regression and wavelet analysis. Atmos. Environ. 74, 346-359. [Google Scholar]

Cheng, S.Y., Li, L., Chen, D.S., Li, J.B. (2012). A neural network-based ensemble approach for improving the accuracy of meteorological fields used for regional air quality modeling. Journal of Environmental Management, 112,404–414. [Google Scholar].

Cigizoglu, H. K., Kisi, O. (2005) Flow prediction by two back propagation techniques using k-fold partitioning of neural network training data. Nordic Hydrol., 36, 1–16. [Google Scholar].

Corporation, H.P. (2013) Forecasting SO_2 pollution incidents by means of Elman artificial neural networks and ARIMA models. Abstr. Appl. Analysis 4, 1728-1749. [Google Scholar].

Djalalova, I., Monache, L.D., Wilczak, J. (2015) $PM_{2.5}$ analog forecast and Kalman filter post-processing for the Community Multiscale Air Quality (CMAQ) model. Atmos. Environ. 108, 76-87. [Google Scholar].

Domannska, D., Woktylak, M. (2012) Application of fuzzy time series models for forecasting pollution concentrations. Expert Syst. Appl. 39, 7673-7679. [Google Scholar]

Elangasinghe, M.A., Singhal N., Dirks, K.N., Salmond J.F. (2014) Development of an ANN–based air pollution forecasting system with explicit knowledge through sensitivity analysis. Atmospheric Pollution Research, 5,696- 708. [Google Scholar].

Feng, X., Li, Q., Zhu, Y., Hou, J., Jin, L., Wang, J. (2015) Artificial neural networks forecasting of PM2.5 pollution using air mass trajectory based geographic model and wavelet transformation. Atmos. Environ. 107, 118-128. [Google Scholar].

Gantt, B., Meskhidze, N., Zhang, Y., Xu, J. (2010) The effect of marine isoprene emissions on secondary organic aerosol and ozone formation in the coastal United States. Atmos. Environ., 44, 115-121. [Google Scholar].

Gao, X.L., Hu, T.J., Wang, K. (2014) Research on motor vehicle exhaust pollution monitoring technology. Appl. Mech. Mater., 620, 244-247. [Google Scholar].

Gardner, M.W., Dorling, S.R. (1998) Artificial neural networks (the multilayer perceptron) a review of applications in the atmospheric sciences. Atmospheric Environment, 32, 2627–2636. [Google Scholar].

Hrust,L.,Klaic,Z.B.,Krizan,J.,Antonic,O.,Hercog,P.(2009) Neural network forecasting of air pollutants hourly concentrations using optimized temporal averages of meteorological variables and pollutant concentrations. Atmospheric Environment

43,5588–5596. [Google Scholar].

Jian, L., Zhao, Y., Zhu, Y.P., Zhang, M., Bertolatti, D. (2012) An application of ARIMA model to predict submicron particle concentrations from meteorological factors at a busy roadside in Hangzhou, China. Sci. Total Environ., 426, 336-345. [Google Scholar].

Jiang, N., Hay, J.E., Fisher, G.W. (2005) Effects of meteorological conditions on concentrations of nitrogen oxides in Auckland. Weather and Climate, 24,15–34. [Google Scholar].

Kurt, A., Oktay, A.B. (2010) Forecasting air pollutant indicator levels with geographic models 3 days in advance using neural networks. Expert Systems with Applications, 37,7986–7992. [Google Scholar]

Lal, S, Patil, R.S. (2001) Monitoring of atmospheric behavior of NOx from vehicular traffic. Environmental Monitoring and Assessment, 68:37–50. [Google Scholar].

Nagendra S.M.S., Khare, M. (2006) Artificial neural network approach for modelling nitrogen dioxide dispersion from vehicular exhaust emissions. Ecological Modelling;190, 99–115. [Google Scholar].

Ozel, G., Cakmakyapan, S. (2015). A new approach to the prediction of PM_{10} concentrations in Central Anatolia Region, Turkey. Atmos. Pollut. Res., 6, 735-741. [Google Scholar].

Pai, T.Y., Hanaki, K., Chiou, R.J. (2013) Forecasting hourly roadside particulate matter in Taipei county of Taiwan based on first-order and one-variable grey model. Cleane Soil Air Water, 41, 737-742. [Google Scholar].

Pauzi, H.M., Abdullah, L. (2015) Neural network training algorithm for carbon dioxide emissions forecast: a performance comparison. Lect. Notes Electr. Eng., 315, 717-726. [Google Scholar].

Perez, P. (2012) Combined model for PM10 forecasting in a large city. Atmospheric Environment, 60, 271–276. [Google Scholar].

Russo, A., Lind, P., Raischel, F., Trigo, R., Mendes, M. (2015). Neural network forecast of daily pollution concentration using optimal meteorological data at synoptic and local scales. Atmos. Pollut. Res., 6 [Google Scholar].

Russo, A., Soares, A.O. (2014) Hybrid model for urban air pollution forecasting: a stochastic spatio-temporal approach. Math. Geosci., 46, 75-93 [Google Scholar].

Samia, A., Kaouther, N., Abdelwahed, T. (2012) A hybrid ARIMA and artificial neural networks model to forecast air quality in urban areas: case of Tunisia. Adv. Mater. Res., 518-523, 2969-2979 [Google Scholar].

Singh, K.P., Gupta, S., Kumar, A., Shukla, S.P. (2012). Linear and nonlinear modeling approaches for urban air quality prediction. Science of the Total Environment, 426,244–255. [Google Scholar].

Urbanski, S.P., Hao, W.M., Nordgren, B. (2011). The wildland fire emission inventory: western United States emission estimates and an evaluation of uncertainty. Atmos. Chem. Phys., 11, 12973-13000. [Google Scholar].

Wang, J., Wang, Y., Liu, H., Yang, Y., Zhang, X., Li, Y., Zhang, Y., Deng, G. (2013). Diagnostic identification of the impact of meteorological conditions on $PM_{2.5}$ concentrations in Beijing. Atmos. Environ., 81, 158-165 [Google Scholar].

Wang, L., Zhang, N., Liu, Z., Sun, Y., Ji, D., Wang, Y. (2014) The influence of climate factors, meteorological conditions, and boundary-layer structure on severe haze pollution in the Beijing-Tianjin-Hebei Region during January 2013. Adv. Meteorol.1-14. [Google Scholar].

Wang, P; Zhang, G., Chen, F., He, Y. (2019). A hybrid-wavelet model applied for forecasting PM2.5 concentrations in Taiyuan city, China. Atmospheric Pollution Research, 10, 1884-1894. [Google Scholar].

Wu, Q., Xu, W., Shi, A., Li, Y., Zhao, X., Wang, Z., Li, J., Wang, L. (2014a) Air quality forecast of PM10 in Beijing with Community Multi-scale Air Quality Modeling (CMAQ) system: emission and improvement. Geosci. Model Dev., 7, 2243-2259. [Google Scholar].

Wu, W., Zha, Y., Zhang, J., Gao, J., He, J. (2014 b) A temperature inversion-induced air pollution process as analyzed from Mie LiDAR data. Sci. Total Environ., 480, 102-108. [Google Scholar].

Yahya, K., Zhang, Y., Vukovich, J.M. (2014) Real-time air quality forecasting over the southeastern United States using WRF/Chem-MADRID: multiple-year assessment and sensitivity studies. Atmos. Environ., 92, 318-338. [Google Scholar].

Yan Chan, K.Y., Jian, L. (2013). Identification of significant factors for air pollution levels using a neural network-based knowledge discovery system. Neurocomputing, 99,564–569 [Google Scholar].

Zhang, Y., Seigneur, C., Bocquet, M., Mallet, V., Baklanov, A. (2012) Real-time air quality forecasting, part I: history, techniques, and current status. Atmos. Environ., 60, 632-655. [Google Scholar].

Zhang, Y., Wang, W., Shao, S., Duan, S., Hou, H. (2017). ANN-GA approach for predictive modelling and optimization of NOx emissions in a cement precalcining kiln. International Journal of Environmental Studies, 74, 253 – 261. [Google Scholar].

Zou, K.H., Tuncali, K.i Silverman, S. G. (2003) Correlation and simple linear regression. Radiology, 227, 617-628. [Google Scholar].